Recovery of Short-Lived Chemical Species in a Couette Flow Reactor

Q. Ouyang and Harry L. Swinney
Center for Nonlinear Dynamics, Department of Physics, University of Texas, Austin, TX 78712

J. C. Roux, P. De Kepper, and J. Boissonade
Centre de Recherche Paul Pascal, Université de Bordeaux I, Chateau Brivazac, F-33600, France

A new technique for studying and recovering short-lived chemical intermediate species has been developed using a Couette reactor, which is an open one-dimensional reaction-diffusion system. Reaction occurs in the annulus between concentric cylinders with the inner one rotating and the outer one at rest. Fresh reagents are in contact with the ends of the annulus, but there is no net axial flow. The axial transport arising from the hydrodynamic motion is effectively diffusive, but has a diffusion coefficient 3 to 5 orders of magnitude larger than that of molecular diffusion. The oxidant (ClO_2^-) and reductant (I^-) of an autocatalytic reaction are fed at opposite ends of the reactor. The reactants diffuse toward each other and react, forming a steady, sharp chemical front and a stable spatial concentration band of unstable intermediate species ($HOCl$) in the front region. Unstable intermediate species are thus stabilized at a well-defined spatial position where they can be recovered and studied. The experiments and numerical simulations demonstrate that the faster the reaction rate, the stabler the chemical front and the more effective the recovery of unstable intermediate species.

Introduction

Stabilization and recovery of unstable intermediate species in a reaction are of interest from both a fundamental and an applied point of view. For example, verification of the existence of short-lived chemical intermediate species may be crucial for developing accurate kinetic models where intermediate species have important roles in the reaction kinetics. From a more applied point of view, the ability to recover a species that would otherwise be short-lived could have important economic consequences. For example, the ability to isolate a particular compound that would otherwise be consumed could lead to the development of new chemical products.

In a continuously-fed, stirred-tank reactor (CSTR), short-lived species may be present in abundance only in certain unstable steady states. Therefore, one way to recover short-lived species would be to maintain a CSTR in an unstable steady state using sophisticated process control strategies, such as feedback control (Aris and Amundson, 1958; Douglas, 1972; Ding et al., 1974; Chang and Schmitz, 1975; Bruns and Bailey, 1975; Laplante, 1989), time-delay feedback control (Zimmerman et al., 1984; Kramer and Ross, 1985; Schell and Ross, 1986), and vibrational control (Meerkov, 1980, 1982; Bellman et al., 1983a,b, 1984a,b; Cinar et al., 1984). In all of these techniques, spatial inhomogeneities are considered unfavorable and are to be avoided.

In contrast, the method described here recovers intermediate species from the *chemical front* region of an inhomogeneous system. In a reaction-diffusion system, two different states, say oxidized and reduced, can appear simultaneously in different parts of the system. Thus, there exist narrow switching regions, chemical fronts, associated with very steep concentration gradients that separate parts of the system corresponding to the different steady-state branches. Since most of the reaction takes place in the narrow front regions, concentrations of unstable intermediate species will be enhanced in these regions and recovery becomes possible.

To keep the chemical front from being destroyed by the recovery flow and to have a reasonable recovery rate, the system requires a much faster diffusive transport process than simple molecular diffusion. This requirement can be fulfilled

Correspondence concerning this article should be addressed to H. L. Swinney.

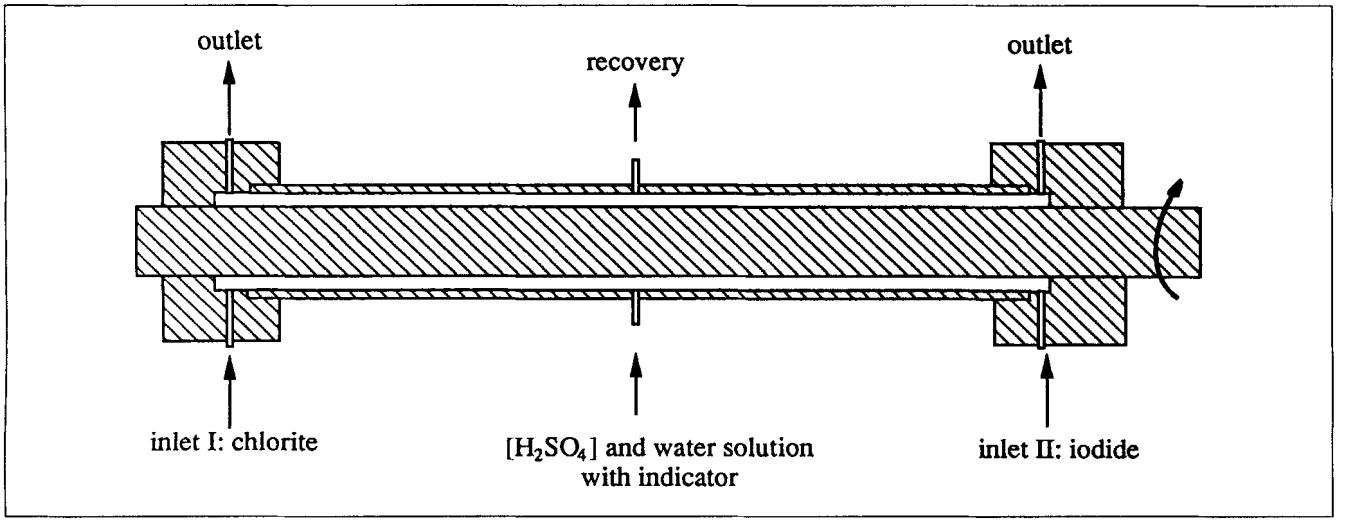

Figure 1. Couette reactor.

The length of the reactor is 120 mm, the diameter of outer cylinder 25.4 mm, and the gap between inner and outer cylinders is 1.59 mm; thus, the ratio of the cylinder radii is 0.875. The reaction occurs in the unshaded region. Diameter of the recovery hole is 1 mm. Inlet solutions contain 5×10^{-3} M of H_2SO_4.

by using a Couette flow reactor, which was developed to study reaction-diffusion instabilities and pattern formation by groups in Texas (Tam et al., 1988; Tam and Swinney, 1990; Vastano et al., 1990; Ouyang et al., 1991) and in Bordeaux (Ouyang et al., 1989, 1991; Boissonade, 1990; De Kepper et al., 1990a; Boissonade et al., 1991). The reactor effectively serves as a one-dimensional reaction-diffusion system with a controllable diffusion rate 3 to 5 orders of magnitude larger than that of molecular diffusion. The use of the Couette reactor to recover intermediate species is described by an experimental and numerical modeling study of recovery of hypochlorous acid from a chlorite-iodide reaction.

Experimental System

Couette reactor

Figure 1 shows a Couette reactor, which consists of two coaxial cylinders of length L, with an inner radius a and an outer radius b. The gap is filled with a reactive fluid of kinematic viscosity ν (0.009 cm^2/s at the experiment temperature of 26°C). The reactor used in this work has $(b-a) \ll b \ll L$. The outer cylinder is fixed while the inner cylinder is rotated at a rate Ω. The flow regime in the gap is determined by the value of the Reynolds number, $Re = (b-a)a\Omega/\nu$. When $Re > Re_c$, the flow self-organizes into pairs of toroidal vortices stacked periodically along the axis (Di Prima and Swinney, 1985). For large rotation rates, $Re \gg Re_c$, the motion becomes turbulent so that the radial and azimuthal mixing are rapidly achieved inside a toroidal cell, and each cell can be considered approximately homogeneous. The axial mass transport from one cell to neighboring ones takes place on much longer time scales than within a cell, and the concentrations can change from one cell to the next. If there is no net axial flow, the total amount of fluid exchanged between two adjacent cells is constant in time and equal in the two opposite directions. Thus, the transport rate of a given species between cells is proportional to the difference of concentration between the two cells, and it can therefore be described by the discretized form of Fick's law. At length scales much larger than the gap width, the system behaves as a quasi-continuum in the axial direction and follows a one-dimensional diffusion law for sufficiently large cylinder rotation rates.

Although the *local* mass transport is achieved by convective turbulent processes of the solvent, the *effective* axial transport is simply diffusive on a scale $L \gg (b-a)$. This has been demonstrated by the experiments of Tam and Swinney (1987) and Ouyang et al. (1991). Furthermore, since turbulence dominates the transport processes, the effective diffusion coefficients D_i for each species i are equal to a single value D, which increases with the rotation rate Ω. In the present experiments, the effective diffusivity D ranges from 0.03 cm^2/s to 0.2 cm^2/s.

To keep fresh chemicals at the boundaries, the reactants are continuously fed and removed at the two ends of the cylindrical gap. The feed and removal flow rates at each end of the Couette reactor are carefully balanced to ensure that the axial mass transport is only diffusive. Recovery was accomplished by opening two small holes in the middle of the reactor: one for continuously recovering chemical solution from the reactor and the other for compensating for the recovery with water with the same pH and concentration of indicator of the recovered solution. The recovery and compensation flow rates are kept equal so that no mass axial flow occurs in the reactor.

Chemical system

A homogeneous liquid reaction was chosen as the chemical system: the minimal chlorite-iodide reaction (Dateo et al., 1982; De Kepper et al., 1990b). The reaction exhibits autocatalytic and substrate inhibition kinetics. Under certain conditions in a batch reactor, it has an induction period with a very slow reaction rate followed by a rapid acceleration, as shown in Figure 2.

In a CSTR with premixed feeds and pH > 1.5, this reaction is bistable between the reduced and oxidized states over a large range of flow rates and concentrations. When the system crosses the transition point, it switches rapidly from one state to the

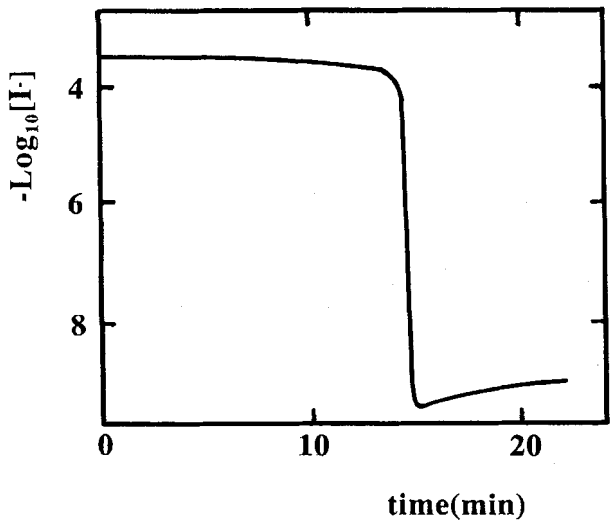

Figure 2. Switching in the chlorite-iodide reaction in a batch reactor.

The long induction period and the subsequent rapid acceleration are shown in this time series of iodide concentration. Initial concentrations: $[H_2SO_4]_i = 5 \times 10^{-3}$ M; $[ClO_2^-]_i = 2.5 \times 10^{-4}$ M; $[I^-]_i = 4.0 \times 10^{-4}$ M. From Dateo et al. (1982).

other. This bistability is observed for ratios of the chlorite-feed to the iodide-feed concentration $[ClO_2^-]_0/[I^-]_0$ in the range 0.2–1.5 (Dateo et al., 1982; Boukalouch et al., 1987); here $[\ ]_0$ refers to the concentration of the mixed reactant stream before any reaction takes place. Figure 3 shows a phase diagram of the bistability.

The reduced and oxidized steady states are optically detectable in the presence of Thiodène (a mixture of urea and starch, an I_3^- indicator, from Prolabo). In this case, the reduced state is blue and corresponds to low light intensity, while

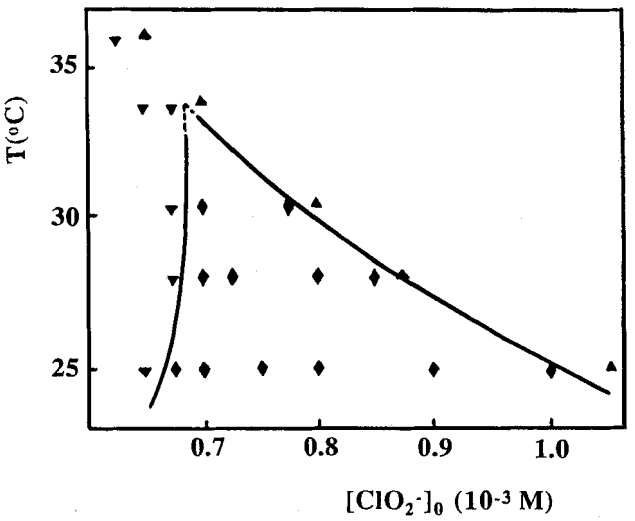

Figure 3. Bistability in the chlorite-iodide reaction in a CSTR.

Measurements show regions of ▼-reduced state; ▲-oxidized state; ♦-oxidation-reduction bistability as a function of temperature and chlorite feed concentration with other feed concentrations held fixed. Fixed concentrations: $[H_2SO_4]_0 = 4.5 \times 10^{-3}$ M; $[Na_2SO_4]_0 = 3.5 \times 10^{-3}$ M; $k_0 = 2.63 \times 10^{-3} s^{-1}$. From Boukalouch et al. (1987).

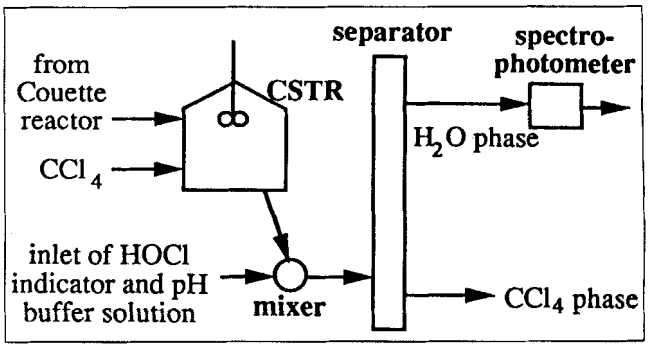

Figure 4. HOCl recovery system.

the oxidized state is yellow and corresponds to high light intensity. The influence of Thiodène on the kinetics of the reaction is negligible when its concentration is less than 0.4 g/L.

Measurement

The state (oxidized or reduced) of the system along the axis of the Couette reactor is monitored with a solid-state video camera. White light is used for illumination. The video camera detects the average transmitted light intensity over a broad spectrum. Therefore, although the measurements indicate the state of the system, they do not yield the concentration of any particular chemical species.

The concentration of one of the intermediate species, hypochlorous acid (HOCl), is measured using the DPD (*N,N*-diethyl-*p*-phenylenediamine) colorimetric method (American Public Health Association, 1975). Although hypochlorous acid remains stable both in an acidic or basic water solution, it is extremely unstable in the chlorite-iodide reaction medium. Thus, it was considered as a unstable intermediate species in the experiments. The main interference in the system for this method is I_2. Since the concentration of I_2 in the system may be ten times greater than that of HOCl, one needs to separate I_2 from HOCl before introducing the indicator. For this reason, carbon tetrachloride (CCl_4) was first added to the recovered solution. Because the solubility of I_2 in CCl_4 is about 100 times larger than that in water, I_2 can be extracted from water solution by CCl_4 with high efficiency. Figure 4 shows the entire on-line measurement procedure. The solution was pumped from the Couette reactor through a recovery hole and immediately mixed with CCl_4 in a small CSTR. The flow rate of CCl_4 was high (500 mL/h) so that the residence time in the CSTR was only about 10 s. After I_2 was extracted, the solution from the CSTR was mixed with the DPD indicator and a pH buffer in a small mixer, where the HOCl reacted with indicator, giving a pink-red color ($\lambda = 552$ nm). The solution was then allowed to separate into a water phase and a carbon tetrachloride phase in a tube. The carbon tetrachloride phase was discarded and the water phase was placed in a spectrophotometer to measure the optical absorption at $\lambda = 552$ nm ($\epsilon = 11{,}000\ M^{-1} \cdot cm^{-1}$). This measurement is relative rather than absolute, since the concentration of HOCl was measured about 10 s after recovery, while reactions that consume or produce HOCl were still under way.

The axial effective diffusion coefficient in this system as function of Ω was measured using the same method as in the

experiments of Tam and Swinney (1987), but for smaller Re/Re_c (3.0-25) than what they studied.

Procedures

The inner cylinder was always accelerated under computer control at the same rate (0.01 rev/s^2) from rest to the final speed. Degassed reductant and oxidant solutions with the same amount of sulfuric acid, sodium sulfate and Thiodène were pumped into separate ends of the reactor, giving an asymmetric feed. The mass flow rate at both ends was kept the same. As will be discussed later, the position of the chemical front in the reactor depends on the ratio of the feed concentration of ClO_2^- to I^-. Therefore, in the recovery process, $[ClO_2^-]_0/[I^-]_0$ was chosen as a tuning parameter to keep the position of the chemical front on the position of the recovery hole or to adjust the relative distance between them. The feed concentration of I^-, the rotation rate Ω, reactant feed flow rate k_0, and recovery flow rate k_r were chosen as the control parameters, while the concentrations of other feed components were fixed: $[H_2SO_4]_0 = 5\times10^{-3}$ M; $[Na_2SO_4]_0 = 3\times10^{-3}$ M; and [Thiodène]$_0$ = 2 g/L. The temperature was fixed at 26°C.

Model and Calculation Method

The chlorite-iodide reaction in the Couette reactor can be described remarkably well by a one-dimensional reaction-diffusion model (Ouyang et al., 1991):

$$\partial c/\partial t = f(c) + D\nabla^2 c$$

with D given by the value of the axial diffusion coefficient in the reactor, and the reaction kinetics $f(c)$ given by the model of Citri and Epstein (1988):

$$H^+ + ClO_2^- + I^- \rightarrow HOCl + HOI \quad (1)$$

$$H^+ + HOI + I^- \rightleftharpoons I_2 + H_2O \quad (2)$$

$$ClO_2^- + HOI + H^+ \rightarrow HIO_2 + HOCl \quad (3)$$

$$HOCl + I^- \rightarrow HOI + Cl^- \quad (4)$$

$$HIO_2 + I^- + H^+ \rightleftharpoons 2HOI \quad (5)$$

$$2HIO_2 \rightarrow HOI + IO_3^- + H^+ \quad (6)$$

$$HIO_2 + HOI \rightarrow I^- + IO_3^- + 2H^+ \quad (7)$$

$$HIO_2 + HOCl \rightarrow IO_3^- + Cl^- + 2H^+ \quad (8)$$

where the rate constant values used were those of Boukalouch et al. (1987):

$$k_{1H} = 2.5\ M^{-1}\cdot s^{-1}$$

$$k_{2H} = 3.57\times10^9\ M^{-1}\cdot s^{-1}$$

$$k_{-2H} = 0.288\ M^{-1}\cdot s^{-1}$$

$$k_{3H} = 6.67\times10^6\ M^{-1}\cdot s^{-1}$$

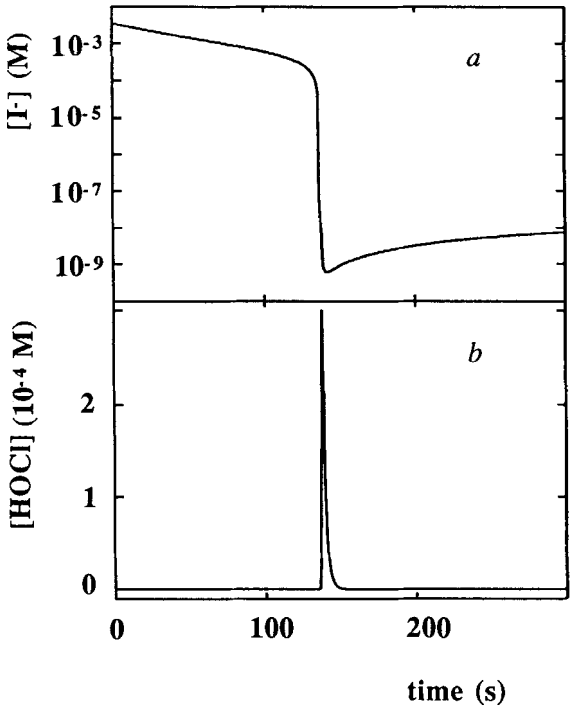

Figure 5. Simulation of I^- and HOCl evolution in a batch reactor.

The calculation used the model of Eqs. 1-8 with initial concentrations: $[ClO_2^-]_i = 2.0\times10^{-3}$ M; $[I^-]_i = 3.5\times10^{-3}$ M.

$$k_4 = 1.4\times10^8\ M^{-1}\cdot s^{-1}$$

$$k_{5H} = 10^4\ M^{-1}\cdot s^{-1}$$

$$k_{-5} = 25\ M^{-1}\cdot s^{-1}$$

$$k_6 = 10^2\ M^{-1}\cdot s^{-1}$$

$$k_7 = 230\ M^{-1}\cdot s^{-1}$$

$$k_8 = 10^3\ M^{-1}\cdot s^{-1}$$

The concentration of H^+ was taken to be 5.0×10^{-3} M (the system was buffered in pH) and hence, was absorbed into the rate constant values k_{iH}.

In the model (Eqs. 1-8), reactions 3 and 4 compose the main loop of the reacting system. This loop is strengthened by reaction 5, where one molecule of HIO_2, the product of Eq. 3, gives two HOI. Therefore, Eqs. 3-5 comprise an autocatalytic loop of the system; HOCl and HOI are autocatalytic species. This autocatalytic loop becomes significant only when the system switches from the reduced state to the oxidized state, where HOCl and HOI exist in a significant amount. In a simulation of the reaction in a batch reactor, one observes an evolution of iodide concentration (Figure 5a), just as in Figure 2, as well as a very sharp peak in the evolution of HOCl (Figure 5b). The lifetime of HOCl is short, about 4 s (see Figure 5b). In a simulation of the reaction in CSTR, a behavior of HOCl similar to that shown in Figure 5b is found when the system undergoes a transition from the reduced state to the oxidized state. Otherwise, the concentration of HOCl is always near zero both in the reduced and oxidized steady states in a CSTR or a batch reactor.

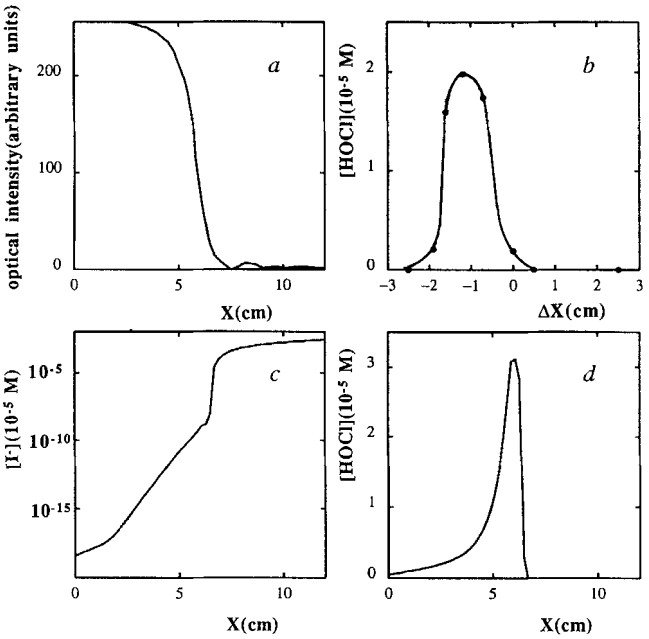

Figure 6. Measurements and simulations of spatial profiles in a Couette reactor.

Results from experiments (a and b) are compared with results from simulations (c and d). a. Scattered light intensity profile of a chemical front structure, $k_0 = 60$ mL/h, $k_r = 0$, and $D = 0.08$ cm^2/s; inlet I, $[ClO_2^-]_0 = 5.0 \times 10^{-3}$ M; inlet II, $[I^-]_0 = 3.5 \times 10^{-3}$ M. b. Measured profile of [HOCl] as a function of the distance ΔX between the recovery point and the chemical front with $k_0 = 100$ mL/h, $k_r = 50$ mL/h, and $D = 0.08$ cm^2/s; inlet I, $[ClO_2^-]_0$ as a tunable parameter; inlet II, $[I^-]_0 = 3.5 \times 10^{-3}$ M. c. Calculated distribution of I^-. d. Calculated distribution of HOCl, with $k_0 = 0.047$ s^{-1}, $k_r = 0$, and $D = 8.0 \times 10^{-3}$ cm^2/s; inlet I, $[ClO_2^-]_0 = 5.0 \times 10^{-3}$ M; inlet II, $[I^-]_0 = 3.5 \times 10^{-3}$ M.

In the Couette flow reactor simulation, the 120-mm-long reactor is modeled as 75 cells, which correspond to the vortices in the real system. The coupling of the cells is assumed to be purely diffusive. Thus, the system obeys the following set of ordinary differential equations:

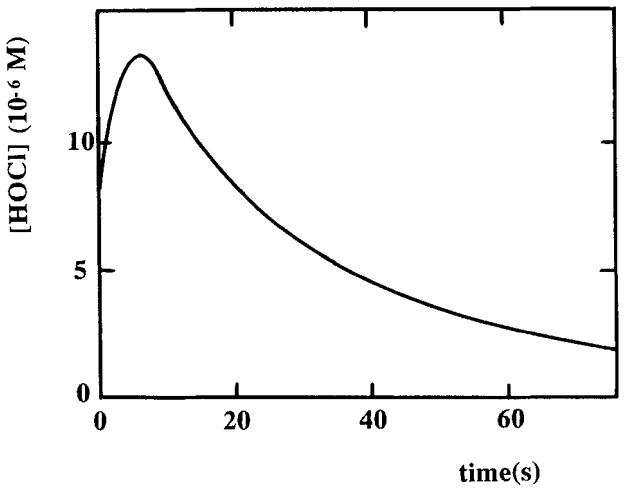

Figure 7. Numerical simulation of the evolution of HOCl in the recovery solution after recovery.

Conditions: $k_0 = 4.2 \times 10^{-3}$ s^{-1}, $k_r = 0.44$ s^{-1}, and $D = 0.008$ cm^2/s; inlet I, $[ClO_2^-]_0 = 5.0 \times 10^{-3}$ M; inlet II, $[I^-]_0 = 3.5 \times 10^{-3}$ M.

$$dC_i/dt = f(C_i) + D(C_{i+1} + C_{i-1} - 2C_i)$$

where $i = 2, \ldots, 74$ (cell number), except for cell j ($j \approx 36$) where the extraction takes place,

$$dC_j/dt = f(C_j) + D(C_{j+1} + C_{j-1} - 2C_j) - k_r C_j,$$

where k_r is the recovery rate. CSTR boundary conditions were applied to the two ends cells:

$$dC_1/dt = f(C_1) + D(C_2 - C_1) + k_0(C_1^0 - C_1)$$

$$dC_{75}/dt = f(C_{75}) + D(C_{74} - C_{75}) + k_0(C_{75}^0 - C_{75}),$$

where k_0 is the flow rate of the CSTRs, and C_i^0 represents feed concentrations of reagents at spatial point i. Because of the large difference in the rate constants for reactions 1 to 8, this system of differential equations is very stiff. Thus, a backward differentiation formula was used in the simulations (formula DEBDF in Shampine and Watts, 1979). The recovery in the Couette reactor was studied in the simulations by putting a recovery hole at the position of the maximum of the [HOCl] distribution. The location of the recovery hole was changed in each step of the calculation so that it followed the location of the maximum [HOCl]. For the chlorite-iodide reaction, the calculations showed that this recovery mode and the recovery mode applied in the experiments give similar results, as long as the chemical front is stable.

Results

Chemical species distributions in the Couette reactor

With appropriate asymmetric feed conditions, the chlorite-iodide reaction in the Couette reactor yields a single stationary front structure. A typical light intensity profile of the structure observed in the experiments is shown in Figure 6a. One can distinguish between an oxidized state region (high light intensity), a reduced state region (low light intensity), and a narrow switching region that represents the chemical front. The position of the chemical front depends on the experimental conditions, and it is particularly sensitive to the ratio $[ClO_2^-]_0/[I^-]_0$. An increase in the ratio will move the front toward the reduced state region, while a decrease will move the front toward the oxidized state region.

The concentration of hypochlorous acid was measured directly for fluid extracted through a small hole midway between the ends of the annulus, as described previously. The numerical simulation shows (Figure 7) that immediately after recovery, the concentration of HOCl first increases, reaches a maximum after about 6 s, and then decreases. This validates the method of determining hypochlorous acid described before, where the measurement is conducted about 10 s after recovery. Of course, the concentration measured in this manner corresponds only roughly to that of the extraction hole (cf. Figure 7).

The spatial profile of hypochlorous acid concentration (Figure 6b) was determined by moving the position of the front relative to the extraction point, which was accomplished by adjusting $[ClO_2^-]_0/[I^-]_0$. The measurements of optical density show that the profile of the front does not change significantly as $[ClO_2^-]_0/[I^-]_0$ is varied over the range necessary to determine the profile of the front.

Figures 6c and 6d show examples of the computed iodide (Figure 6c) and hypochlorous acid (Figure 6d) concentration profiles. The iodide concentration changes by several orders

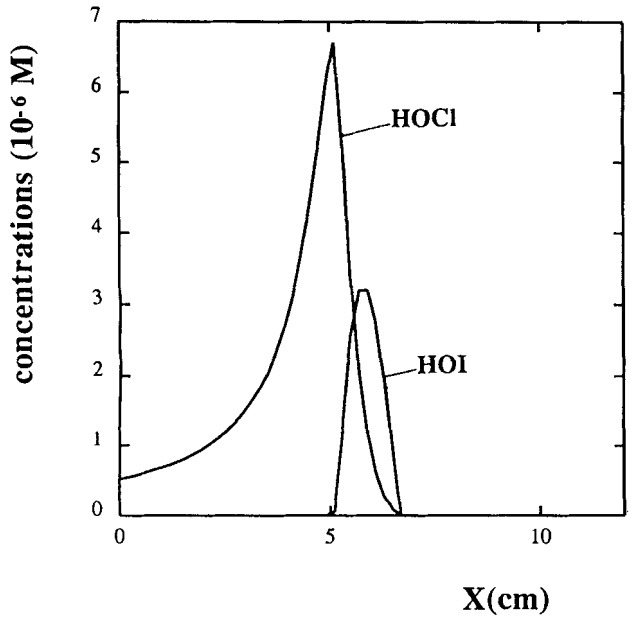

Figure 8. Simulations of HOCl and HOI concentration profiles in a Couette reactor.

Conditions: $k_0 = 0.047\ s^{-1}$, $k_r = 0$, and $D = 8.0 \times 10^{-3}\ cm^2/s$; inlet I, $[ClO_2^-]_0 = 5.0 \times 10^{-4}$ M; inlet II, $[I^-]_0 = 3.5 \times 10^{-4}$ M.

of magnitude in the narrow steady chemical front. This drop in iodide concentration corresponds to the change of color from blue to yellow, as observed in the experiment. Thus, the iodide concentration profile obtained from the simulation (Figure 6c) can be compared directly to the profile of optical intensity observed in the experiment (Figure 6a). In Figure 6d one observes, as in Figure 6b, a narrow spatial band of hypochlorous acid concentration in the chemical front region. This agreement between the experimental and numerical result demonstrates that the one-dimensional reaction-diffusion model qualitatively captures the spatial concentration profile of the Couette reactor system, even though fast complex reactions are involved.

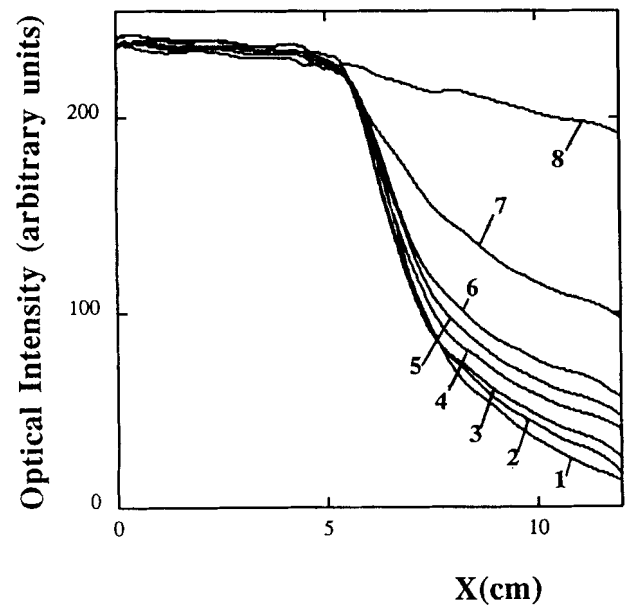

Figure 9. Measured intensity profiles for different recovery flow rates.

These measurements show the collapse of the chemical front with increasing flow rate. Recovery flow rates (in mL/h): (1) $k_r = 0$, (2) $k_r = 20$, (3) $k_r = 40$, (4) $k_r = 80$, (5) $k_r = 120$, (6) $k_r = 160$, (7) $k_r = 200$, (8) $k_r = 240$. Other control parameters were: $k_0 = 20$ mL/h, and $D = 0.03\ cm^2/s$; inlet II; $[I^-]_0 = 1.0 \times 10^{-3}$ M; inlet I, $[ClO_2^-]_0$, a tunable parameter.

A comparison of the experimental results of Figure 2 with Figure 6a and the numerical simulations of Figure 5 with Figures 6c and 6d indicates that the Couette reactor can stabilize states that would be transient in a batch reactor or a CSTR. In a certain sense, the Couette reactor converts the *temporal* evolution of reactive species in a batch reactor into *spatial* concentration distributions. The unstable species in a batch reactor or CSTR, such as hypochlorous acid, can thus be easily stabilized in the chemical front in a Couette reactor and can be recovered as a chemical product. Moreover, as shown in the numerical simulation of Figure 8, the maximum of each unstable species has a different spatial location in the Couette reactor. Therefore, one can change the recovery position or, more simply, change the front position to get maximum productivity and better selectivity for a desired intermediate species.

Stability of chemical front under recovery

Clearly, the ideas presented above are applicable only if the chemical front persists under recovery. Therefore, the stability of the chemical front was studied as a function of the recovery rate. Figure 9 shows light intensity profiles for different recovery flow rates in the experiments. The chemical front persists for large recovery flow rates, but the gradient of the front becomes smaller as the recovery flow rate increases. Eventually, the recovery flow rate passes a critical point and the front structure collapses, giving rise to a quasi-homogeneous state. Within the experimental uncertainty, no hysteresis was found in this experiment.

The influence of recovery on the concentration of hypochlorous acid as a function of the distance (ΔX) between front and recovery positions is shown in Figure 10. In the front structure, an increase in the recovery flow rate causes a decrease in the maximum concentration of hypochlorous acid. After the chemical front collapsed, no hypochlorous acid was detected in the experiments. This finding is supported by numerical simulations (Figure 11). Note that the maximum in the hypochlorous acid concentration suddenly drops several orders of magnitude when the chemical front collapses. Consequently, the idea of recovering unstable short-lived intermediate species near a chemical front in a Couette reactor is feasible, provided that the recovery flow rate is not so large that the chemical front collapses.

The critical value of the recovery flow rate depends on other control parameters: it increases with increasing reactor feed rates or increasing feed concentrations. The effect of the diffusion rate is complex. According to the numerical simulations, an increase in the diffusion coefficient stabilizes the front structure. Moreover, if the diffusion rate is large enough, a change of diffusion coefficient will not change the critical value of the recovery flow rate. The diffusion values in this experiment were sufficiently large ($D = 0.03$ to $0.2\ cm^2/s$), so that the critical value of the recovery flow was fairly insensitive to the value of D.

The diffusion coefficient, however, is an important control

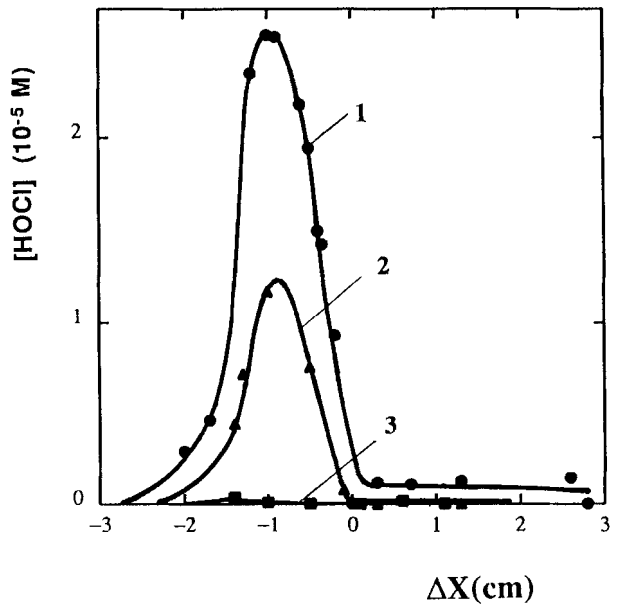

Figure 10. Measured effect of recovery rate on the spatial distribution of HOCl in the Couette reactor.

The curve shows [HOCl] in the recovery system as a function of the distance of the front from the hole. The position of the front is varied by tuning $[ClO_2^-]_0$. Conditions: (1) $k_r = 127$ mL/h, (2) $k_r = 252$ mL/h, (3) $k_r = 400$ mL/h, with $k_0 = 100$ mL/h, and $D = 0.03$ cm^2/s; inlet II, $[I^-]_0 = 1.32 \times 10^{-3}$ M.

parameter because the shape and maximum value of the hypochlorous acid concentration distribution depend on D. Figure 12a shows experimental data for the hypochlorous acid concentration as a function of distance (ΔX) between the front and recovery point for different values of the diffusion coefficient. Figure 12b gives the results for the corresponding numerical simulation. With the other control parameters kept constant, an increase in the diffusion coefficient both increased the maximum concentration and enlarged the width of the hypochlorous acid distribution band. Therefore, to increase productivity and to control the system better, it is better to operate a Couette reactor with a high diffusion coefficient (large rotation rates of the cylinder).

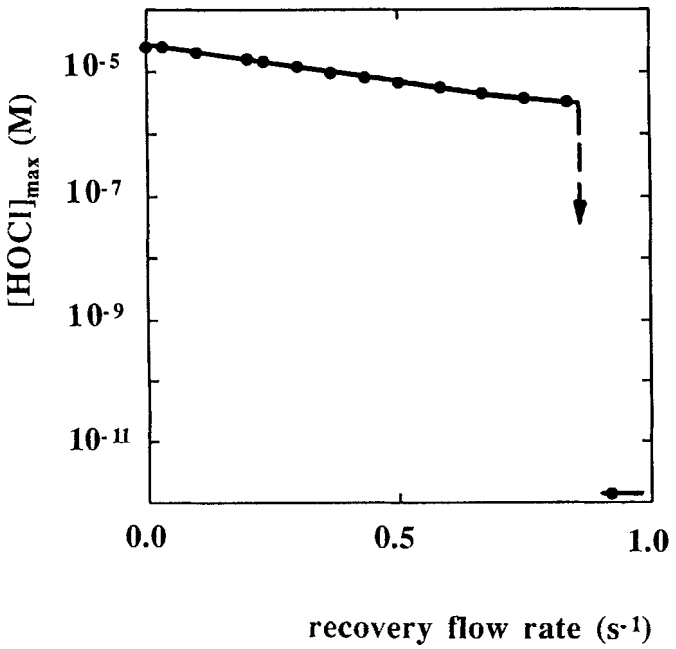

Figure 11. Calculated effect of recovery rate on the maximum of HOCl concentration.

Other control parameters were: $k_0 = 4.2 \times 10^{-3}$ s^{-1}, $D = 8 \times 10^{-3}$ cm^2/s; inlet I, $[ClO_2^-]_0 = 5.0 \times 10^{-3}$ M; inlet II, $[I^-]_0 = 3.5 \times 10^{-3}$ M.

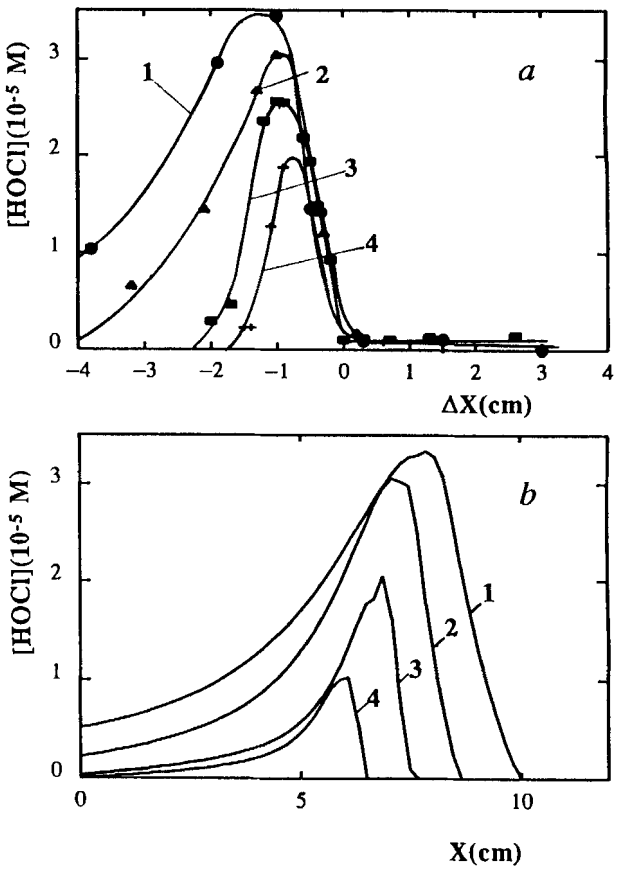

Figure 12. Influence of diffusion coefficient on the HOCl distribution determined in (a) experiments and (b) simulations.

a. (1) $D = 0.2$ cm^2/s, (2) $D = 0.14$ cm^2/s, (3) $D = 0.08$ cm^2/s, (4) $D = 0.03$ cm^2/s, with $k_0 = 100$ mL/h, and $k_r = 50$ mL/h; inlet II, $[I^-]_0 = 1.3 \times 10^{-3}$ M; inlet I, $[ClO_2^-]_0$ a tunable parameter.
b. (1) $D = 0.2$ cm^2/s, (2) $D = 0.08$ cm^2/s, (3) $D = 0.02$ cm^2/s, (4) $D = 0.008$ cm^2/s, with $k_0 = 0.067$ s^{-1}, $k_r = 0.25$ s^{-1}; inlet I, $[ClO_2^-]_0 = 2.5 \times 10^{-3}$ M; inlet II, $[I^-]_0 = 1.4 \times 10^{-3}$ M.

Efficiency of recovery

To evaluate the Couette reactor for industrially important situations, the product flow rate and productivity were calculated in the system. Since one mole of chlorite can convert a maximum of one mole of hypochlorous acid, one can take $k_r[HOCl]_r$ as the value of the product flow rate and $k_r[HOCl]_r/(k_0[ClO_2^-]_0)$ as the value of productivity, where k_0 and k_r are the feed and recovery flow rates, respectively. The terms $[ClO_2^-]_0$ and $[HOCl]_r$ represent the feed concentration of chlorite and the recovery concentration of hypochlorous acid.

The results of the numerical simulation for the product flow rate and productivity are presented in Figure 13 as a function

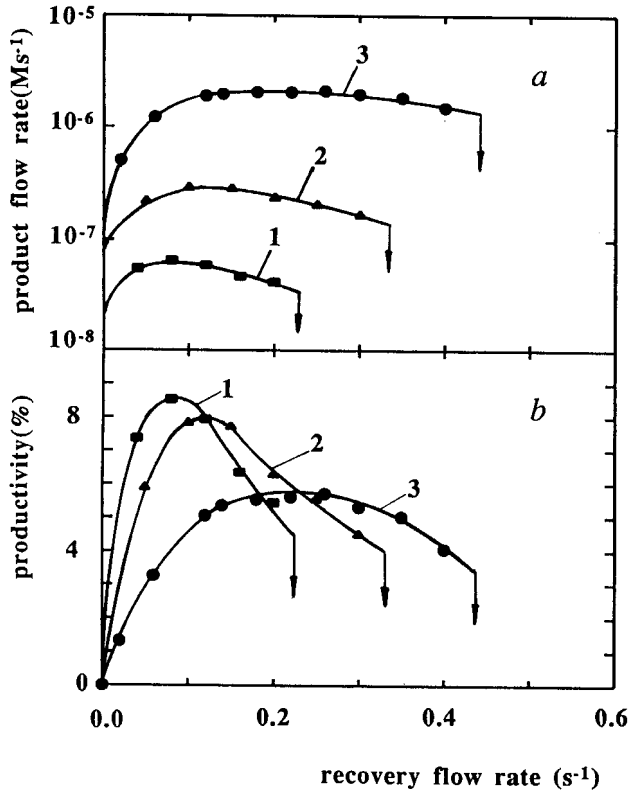

Figure 13. Simulations of product flow rate and productivity on recovery flow rate.

The product flow rate k_r[HOCl], and productivity k_r[HOCl]$_r$/$k_0[ClO_2^-]_0$ were computed for the following conditions: (1) $[I^-]_0 = 3.5\times10^{-3}$ M, (2) $[I^-]_0 = 3.5\times10^{-4}$ M, (3) $[I^-]_0 = 7\times10^{-5}$ M, with $[ClO_2^-]_0/[I^-]_0 = 1.43$, $k_0 = 4.2\times10^{-3}$ s^{-1}, $D = 0.008$ cm^2/s.

of recovery flow rate for different chlorite feed concentrations. In the front structure the productivity is relatively high, and there exists an optimal value of the recovery flow rate corresponding to the maximum productivity. A decrease in the feed concentration of chlorite will increase the productivity. This increase in productivity, however, is accompanied by a decrease in the product flow rate. Similarly, a decrease in the feed flow rate at the ends of the Couette reactor will also increase the productivity and decrease the product flow rate. Calculations show that it is possible to obtain up to 20% productivity if one uses a very small input flow ($k_0[ClO_2^-]_0$).

Discussion

The Couette reactor provides a novel means of recovering short-lived, unstable intermediate species, which can be locally abundant in a chemical front in the reactor. Recovery of short-lived species is extremely difficult in a batch reactor as well as in a CSTR; in the latter one must use a sophisticated control process to maintain the system in an unstable state. In both cases, the desired species is uniformly mixed with all other species. In contrast, since species are separated in a Couette reactor, the chemical composition of the recovery solution in a Couette reactor can be very different from that of the solution in a batch reactor at the point when the unstable species become abundant.

A major difference also exists between the Couette and plug flow reactors: in plug flow the reactants must be premixed, while in a Couette reactor the reactants can be separated (in the example considered here, chlorite is fed from one end while iodide is fed from the other end). This separation of reactants could be crucial for work with fast reactions.

Three principal factors determine the stability of a chemical front under recovery in the Couette reactor: the mass transport rate, the reaction rate, and the recovery rate. The first two strengthen the chemical front, while the latter one tends to destroy it. In a reaction-diffusion system with only molecular diffusion, the recovery of intermediate species would be limited by the mass transport rate, and a small perturbation in the recovery rate would easily destroy the front. In a Couette reactor, however, the enhanced diffusion rate is much larger than the molecular diffusion rate, and it is possible to adjust the diffusion rate such that the transport process is not the rate-limiting step. Consequently, there are two competitors left: the reaction rate and the recovery rate. If the reaction rate is larger than the recovery rate, the front survives and recovery with enhanced yield can be achieved; this is not possible if the recovery rate is larger than the reaction rate so that the front collapses. One thus comes to a very interesting conclusion: in contrast to the situation in a batch reactor, a CSTR, or a plug flow reactor, where the higher the reaction speed, the more difficult it is to isolate an intermediate species, in the Couette reactor the faster the reaction rate, the stabler the chemical front and the more efficient the recovery of the unstable short-lived intermediate species! The experiments and numerical simulations with the chlorite-iodide reaction system presented in this work support the above conclusion.

Another important feature of the Couette reactor is that the effective diffusion coefficient can be controlled. For example, in cases where the reaction rate of the intermediate species is so fast that the spatial distribution of the species is too narrow to resolve, one can increase the diffusion coefficient of the reactor (by increasing the rotation rate of the inner cylinder) to spread out the distribution band.

In this study, an autocatalytic reaction was used to demonstrate the new technique, which in principle can be applied to other reaction systems. Potential applications of this technique range from detecting intermediate products and studying the mechanism of a fast reaction to making new chemical products. For example, polymerization reaction products with a desired molecular weight could be obtained in a Couette reactor by recovering them from the appropriate location along the length of the reactor.

More theoretical as well as experimental work is needed to understand the chemical front structures, the spatial distributions of intermediate species, the stability of the fronts with imposed gradients in concentration, temperature, or light intensity, and the relative merits of the Couette and plug-flow reactors in diverse applications.

Acknowledgment

We would like to acknowledge fruitful discussions with W. D. McCormick, Z. Noszticzius, G. Kshirsagar, and R. Dennis Vigil. This work is supported by a grant from BP Venture Research.

Notation

a = inner radius of Couette reactor, cm
b = outer radius of Couette reactor, cm

C_i = vector of chemical concentrations in the spatial point i, M(mol/L)
C_i^0 = vector of feed concentrations of reagents to spatial point i, M(mol/L)
D = axial effective diffusion coeffcient in the Couette reactor, cm^2/s
D_i = diffusion coefficient of chemical species i, cm^2/s
k_0 = feed flow rate of reactant, s^{-1}
k_r = recovery flow rate, s^{-1}
K_i = rate constant of reaction i
K_{iH} = rate constant of reaction i including acid concentration (constant, 5×10^{-3}M)
L = length of Couette reactor, cm
MW = molecular weight, g
Re = Reynolds number, $(b-a)a\Omega/\nu$
Re_c = Reynolds number corresponding to the primary instability, 118.2
T = temperature, °C
ΔX = distance between positions of recovery point and chemical front, cm
$[\ ]_0$ = feed concentration of reagents before any reaction takes place, M(mol/L)
$[\ ]_r$ = concentration of product in the recovery point, M(mol/L)

Greek letters

ϵ = absorption coefficient, $M^{-1}\cdot cm^{-1}$
λ = light wavelength, nm
ν = kinematic viscosity, cm^2/s
Ω = rotation speed of inner cylinder of Couette reactor, s^{-1}

Literature Cited

American Public Health Association, *Standard Methods for the Examination of Water and Wastewater*, p. 304, Washington, DC (1975).

Aris, R., and N. R. Amundson, "An Analysis of Chemical Reactor Stability and Control," *Chem. Eng. Sci.*, **7**(3), 121 (1958).

Bellman, R., J. Bentsman, and S. M. Meerkov, "Vibrational Control of Systems with Arrhenius Dynamics," *J. Math. Anal. Appl.*, **91**, 152 (1983a).

Bellman, R., J. Bentsman, and S. M. Meerkov, "Nonlinear Systems with Fast Parametric Oscillations," *J. Math. Anal. Appl.*, **97**, 572 (1983b).

Bellman, R., J. Bentsman, and S. M. Meerkov, "Vibrational Stabilizability of Nonlinear Systems," *Proc. World IFAC Cong.*, **8**, 53, Budapest (1984a).

Bellman, R., J. Bentsman, and S. M. Meerkov, "Vibrational Control of Nonlinear Systems," *Proc. Control Decision Conf.*, **1**, 84, Las Vegas (1984b).

Boissonade, J., "Sustained Chemical Dissipative Structures. Some Recent Developments," *Dynamics and Stochastic Processes: Theory and Application*, K. Lima, L. Streit, and R. Vilela Mendes, eds., Lecture Notes in Physics, No. 355, 1976, Springer (1990).

Boissonade, J., Q. Ouyang, A. Arneodo, J. Elezgaray, J. C. Roux, and P. De Kepper, "Sustained Reaction-Diffusion Waves and Stationary Structures in an Open Reactor," *Nonlinear Wave Processes in Excitable Media*, p. 47, A. V. Holden, M. Markus, and H. G. Othmer, eds., Pergamon Press (1991).

Boukalouch, M., J. Boissonade, and P. De Kepper, "Du Mélange Imparfait à la Structure Spatiotemporelle: Oscillations Induites par l'Inhomogénété dans la Réaction Chlorite-Iodure," *J. Chim. Physique*, **84**, 1353, France (1987).

Bruns, D. D., and J. E. Bailey, "Process Operation Near an Unstable Steady State Using Nonlinear Feedback Control," *Chem. Eng. Sci.*, **30**, 775 (1975).

Chang, M., and R. A. Schmitz, "Feedback Control of Unstable States in a Laboratory Reactor," *Chem. Eng. Sci.*, **30**, 837 (1975).

Cinar, A., J. Deng, S. M. Meerkov, and X. Shu, "Vibrational Control of an Exothermic Reaction in a CSTR: Theory, Simulation, Experiment," *AIChE Meeting*, San Francisco, Paper No. 101b (1984).

Cinar, A., J. Deng, S. M. Meerkov, and X. Shu, "Vibrational Control of an Exothermic Reaction in a CSTR: Theory and Experiments," *AIChE J.*, **33**, 353 (1987).

Citri, O., and I. R. Epstein, "Mechanistic Study of a Coupled Chemical Oscillator. The Bromate-Chlorite-Iodide Reaction," *J. Phys. Chem.*, **92**, 1856 (1988).

Dateo, C. E., M. Orbàn, P. De Kepper, and I. R. Epstein, "Bistability and Oscillations in the Autocatalytic Chlorite-Iodide Reaction in a Stirred-Flow Reactor," *J. Amer. Chem. Soc.*, **104**, 504 (1982).

De Kepper, P., Q. Ouyang, J. Boissonade, and J. C. Roux, "Sustained Coherent Spatial Structures in a Quasi-1D Reaction-Diffusion System," *Dynamics of Exotic Phenomena in Chemistry*, H. Beck and B. Koros, eds., *Reac. Kinet. Catal. Lett.*, **42**, 275 (1990a).

De Kepper, P., J. Boissonade, and I. R. Epstein, "Chlorite-Iodide Reaction: A Versatile System for the Study of Nonlinear Dynamical Behavior," *J. Phys. Chem.*, **95**, 6525 (1990b).

Ding, J. S. Y., S. Sharma, and D. Luss, "Steady State Multiplicity and Control of the Chlorination of Liquid *n*-decane in an Adiabatic CSTR," *Ind. Eng. Chem. Fundam.*, **13**(1), 76 (1974).

DiPrima, C., and H. L. Swinney, *Hydrodynamic Instabilities and Transition to Turbulence*, H. L. Swinney and J. P. Gollub, eds., Chap. 6, Springer (1985).

Douglas, J. M., *Process Dynamics and Control*, Prentice-Hall, Englewood Cliffs, NJ (1972).

Kramer, J., and J. Ross, "Stabilization of Unstable States, Relaxation, and Critical Slowing Down in a Bistable System," *J. Chem. Phys.*, **83**(12), 6234 (1985).

Laplante, J. P., "Stabilization of Unstable States in the Bistable Iodate-Arsenous Acid Reaction in a Continuous Flow Stirred Tank Reactor," *J. Phys. Chem.*, **93**, 3882 (1989).

Meerkov, S. M., "Principle of Vibrational Control: Theory and Applications," *IEEE Trans. Auto. Control*, **AC-25**(4), 755 (1980).

Meerkov, S. M., "Condition of Vibrational Stabilizability for a Class of Nonlinear Systems," *IEEE Trans. Auto. Control*, **AC-27**(2), 485 (1982).

Ouyang, Q., J. Boissonade, J. C. Roux, and P. De Kepper, "Sustained Reaction-Diffusion Structures in an Open Reactor," *Phys. Lett. A*, **134**, 284 (1989).

Ouyang, Q., V. Castets, J. Boissonade, J. C. Roux, P. De Kepper, and H. L. Swinney, "Sustained Patterns in Chlorite-Iodide Reactions in a One-dimensional Reactor," *J. Chem. Phys.*, **95**, 351 (1991).

Schell, M., and J. Ross, "Effects of Time Delay in Rate Processes," *J. Chem. Phys.*, **85**, 6489 (1986).

Shampine, L. F., and H. A. Watts, "DEPAC—Design of a User Oriented Package of ODE Solvers," SAND79-2374, Sandia Laboratories (1979).

Tam, W. Y., and H. L. Swinney, "Mass Transport in Turbulent Couette-Taylor Flow," *Phys. Rev. A*, **36**, 1374 (1987).

Tam, W. Y., J. A. Vastano, H. L. Swinney, and W. Horsthemke, "Regular and Chaotic Chemical Spatiotemporal Patterns," *Phys. Rev. Lett.*, **61**, 2163 (1988).

Tam, W. Y., and H. L. Swinney, "Spatiotemporal Patterns in an One-Dimensional Open Reaction-Diffusion System," *Physica D*, **46**, 10 (1990).

Vastano, J., T. Russo, and H. L. Swinney, "Bifurcation to Spatially Induced Chaos in a Reaction-Diffusion System," *Physica D*, **46**, 23 (1990).

Zimmermann, E. C., M. Schell, and J. Ross, "Stabilization of Unstable States and Oscillatory Phenomena in an Illuminated Thermochemical System: Theory and Experiment," *J. Chem. Phys.*, **81**, 1327 (1984).

Manuscript received June 27, 1991, and revision received Jan. 21, 1992.